Am J Transl Res 2021;13(5):4412-4421
www.ajtr.org /ISSN:1943-8141/AJTR0116100

Original Article

Sphingomyelin synthase 2 but not sphingomyelin synthase 1 is upregulated in ovarian cancer and involved in migration, growth and survival via different mechanisms

Fang Jing[1], Chao Jing[2], Xiaoyan Dai[3], Guang Zhou[3], Shi Di[3], Xiaoxia Bi[3], Tingting Dai[4], Tingting Qin[5], Li Hong[1]

[1]Department of Gynaecology, Renmin Hospital of Wuhan University, Wuhan, China; [2]Department of Stomatology, Cangbu Central Hospital of Xinzhou District, Wuhan, China; [3]Department of Gynaecology, Tongren Hospital of Wuhan University (Wuhan Third Hospital), Wuhan, China; [4]Department of Obstetrics, Tongren Hospital of Wuhan University (Wuhan Third Hospital), Wuhan, China; [5]Department of Integrated Chinese and Western Medicine, Tongren Hospital of Wuhan University (Wuhan Third Hospital), Wuhan, China

Received June 11, 2020; Accepted February 21, 2021; Epub May 15, 2021; Published May 30, 2021

Abstract: Sphingomyelin synthase 1 (SMS1) and 2 (SMS2) are two enzymes required for sphingomyelin *de novo* synthesis, and their roles in tumor transformation and development have been recently recognized. In this work, we systematically evaluated the expression patterns of SMS1 and 2 in ovarian cancer patient samples and cell lines. Furthermore, we analyzed the functions of SMS2 and its underlying mechanisms. We observed a specific increase in SMS2 expression in ovarian cancer tissues compared to the adjacent normal ovary tissues in majority of patients' samples. This is regardless of their clinico-pathological characteristics. SMS1 expression was similar between ovarian cancer and its normal counterpart in 30 patients tested. The upregulation of SMS2 but not SMS1 was also reproducible in a panel of ovarian cancer cell lines. Functional analysis indicated that SMS2 plays a predominant role in promoting migration rather than proliferation in ovarian cancer. SMS2 depletion suppressed migration, growth and survival, and furthermore this was dependent on SMS2 baseline level in ovarian cancer cells. SMS2 inhibition significantly augmented cisplatin's efficacy. We further found that migration inhibition induced by SMS2 depletion was largely due to the suppression of RhoA/ROCK/LIMK/cofilin and RhoA/ROCK/FAK/paxillin pathways. In addition, lipid metabolism disruption, oxidative stress and damage, and impaired mitochondrial function contributed to the inhibitory effects of SMS2 depletion in ovarian cancer growth and survival. Our work demonstrates that SMS2 but not SMS1 is upregulated in ovarian cancer and involved in migration, growth and survival via different mechanisms. Our findings highlight the therapeutic value of SMS2 inhibition in the treatment of ovarian cancer.

Keywords: Ovarian cancer, sphingomyelin synthase, RhoA signaling, oxidative stress, cisplatin

Introduction

Ovarian cancer is the seventh most common malignancy worldwide and is associated with the highest mortality rate among gynecological malignancies [1]. Based on the histopathological and genomic differences, ovarian cancer is divided into five subtypes with high grade serious ovarian cancer (SOC) and ovarian clear cell carcinoma (OCCC) as the two most common subtypes [2]. Although there have been recent advances in the treatment of some gynecological malignances, ovarian cancer therapy has remained essentially unchanged for over 30 years. Ovarian cancer is more frequently diagnosed at advanced stage, and majority of patients will inevitably relapse, due to treatment resistance. This is despite of their initial response to platinum-based chemotherapy [3, 4]. Thus, further research is warranted to develop complementary therapeutic strategies for treating this disease.

Sphingomyelin (SM) biosynthesis, a complex and finely regulated process, which links to lipid metabolism and signal transduction, has emerged as an intriguing therapeutic target in cancer [5, 6]. Of note, emerging data showed

the regulation of sphingolipid metabolism contribute to resistance for platinum-based agents in ovarian cancer [7]. SM biosynthesis is carried out by two enzymes, sphingomyelin synthase 1 (SMS1) and 2 (SMS2). Both enzymes utilize phosphatidylcholine (PC) and ceramide to produce SM and diacylglycerol (DAG) [8]. The role of SMS2 in regulating cancer development has been revealed but are inconclusive. Some studies demonstrate the pro-cancer activity of SMS2 by showing that SMS2 promotes an aggressive breast cancer phenotype [9] and glioblastoma patients with low SMS2 expression have a higher 5-year survival than those with high SMS2 expression [10]. In contrast, SMS2 overexpression promotes cisplatin-induced apoptosis of hepatocellular carcinoma cells [11], suggesting the anti-cancer activity of SMS2. Here, we systematically analyzed expression pattern of SMS1 and SMS2 in ovarian cancer patient samples and cell lines to understand the overall trends of both targets. Next, we focused on evaluating the role of SMS2 and its underlying mechanisms in preclinical ovarian cancer models.

Materials and methods

Patient tissue samples and cell lines

Malignant and normal ovarian samples were obtained from patients seen at Renmin Hospital of Wuhan University. Informed consent was obtained from each patient and protocols for patient recruitment were approved by the institutional research ethics committees. Patient demographics were summarized in Supplementary Table 1. Seven human ovarian cancer cell lines (The Cell Bank of the Chinese Academy of Sciences) and one immortalized human ovarian epithelial cell line (IHOEC, Creative Bioarray) were maintained in Dulbecco's modified Eagle's medium (DMEM; HyClone) supplemented with 10% fetal bovine serum (FBS; HyClone) and 1% penicillin/streptomycin (Invitrogen). The ovarian cell lines were authenticated by short tandem repeat profiling (XP Biomed).

Immunohistochemistry and western blot analysis

Snap frozen tissues were sectioned with a cryostat, fixed with 10% paraformaldehyde (Sigma) and washed with PBS. The sections were stained with 1:500 dilution of anti-SMS1 or anti-SMS2 antibodies (Abcam) overnight at 40°C, and then incubated with designated 2nd antibodies conjugated with HRP for 2 hr at room temperature. Signals were developed using DAB (3, 3'-diaminobenzidine) staining kit (Abcam) and visualized under light microscope. Sections were also counterstained with haematoxylin. Total protein was extracted using RIPA buffer and quantified using BCA protein assay kit (Thermofisher). Protein was loaded onto SDS-PAGE gel and resolved by electrophoresis prior to western blot analysis using standard protocol. Antibodies against active and total Rac and RhoA, phosphor and total MYPT1, cofilin and PRK2 were obtained from Cell signalling.

ELISA assays

The quantification of SMS1 and SMS2 in tissue and cells were determined using Human sphingomyelin synthase 1 and Human sphingomyelin synthase 2 ELISA kits (MyBioSource). Antibody specific for SMS1 or SMS2 has been pre-coated onto a microplate and this ELSIA assay employs the quantitative sandwich enzyme immunoassay technique. Cell lysates and tissue homogenates were prepared according to manufacturer's instructions. The quantifications of RhoA and Rac1 activities in cells were determined using RhoA G-LISA Activation Assay kit and Rac1 G-LISA Activation Assay kit (Cytoskeleton) as per the manufacturer's protocol.

Proliferation assay

5000 cells/well were seeded onto a 96-well-plate and incubated with cisplatin (Selleck) for 3 days. Cell proliferation was evaluated using BrdU Proliferation Assay Kit (Cell Signaling).

Apoptosis assay

10^6 cells/well were seeded onto a 12-well-plate and incubated with cisplatin for 3 days. Cells were detached using trypsin and stained with Annexin V-FITC/7-AAD (BD Pharmingen) as per manufacturer's protocol. After staining, cells were processed on MACSQuant flow cytometer and analyzed using the MACSQuantify Software. Annexin V (+)/7-AAD (-) and Annexin V (+)/7-AAD (+) were considered as apoptotic cells.

Transwell migration assay

10^4 cells/well with or without cisplatin were seeded onto the upper chambers of a transwell plate. 2% FBS and 10% FBS were placed into upper and lower chamber, respectively. After 12 hr incubation, the cells spreading on the upper surfaces of the filter (non-migrated cells) were wiped away with cotton swabs, and the migrated cells on the lower surface of the filter were fixed, stained with Giemsa (Sigma). Migrated cells from five random fields per well were counted under the light microscope.

Transfection

Transfection was performed using Dharmafect transfection reagent on 10^6 cells/well in a 6-well-plate according to manufacturer's instructions. For SMS2 overexpression, SMS2 was cloned into pcDNA5/FRT mammalian expression vector (Thermofisher). For SMS2 siRNA knockdown, two siRNA that target different regions of SMS2 and scramble control were obtained from GenePharma and the sequences were summarized in Supplementary Table 2.

RT-PCR

Total RNA was isolated from cells using the TRIzol (Invitrogen). The first-strand cDNA was synthesized by using iScript cDNA Synthesis Kit (Bio-rad). PCR was performed using a SsoFast EvaGreen Supermix on CFX96 RT PCR system (Bio-rad). The primers for SMS1 and SMS2 were listed in Supplementary Table 3.

Lipid measurement

Ceramide, phosphatidylcholine (PC) and sphingomyelin (SM) levels were quantified using a liquid chromatography mass spectrometry (LC-MS) system (Prominence, Shimazu and 4000 QTrap, Applied Biosystems) according to the procedures described previously [12]. Briefly, cells were lysed using the Precellys Homogeniser. Samples for ceramide analysis were spiked with isotope-labeled 16:0, 18:0 and 24:0 ceramides and samples for PC and SM analyses were spiked with 14:0, 14:0 PC and 17:0 SM internal standards prior to extraction. For lipid extraction, 20 µL of lipid internal standard mix, 10 µl of phosphatidylcholine and 1.2 ml of HPLC grade methanol were added to lysates prior to spinning down. The sample extracts were reconstituted in 500 µl methanol before analysis using a LC-MS.

Measurement of mitochondrial membrane potential, reactive oxygen species (ROS) and oxidative DNA damage

To measure mitochondrial potential, cells were stained with 5,5',6,6'-tetrachloro-1,1',3,3'-tetraethyl benzimidazolylcarbocyanine iodide (JC-1, Invitrogen) according to manufacturer's instructions and analyzed on MACSQuant flow cytometer for JC-1 level. To detect ROS, cells were incubated with 10 µM CM-H_2DCFDA (Life Technologies, US) at 37°C for 1 hr. The absorbance at ex/em of 495/525 nm was measured using Spectramax M5 microplate reader (Molecular Devices). To measure oxidative DNA damage, 8-hydroxy-2'-deoxyguanosine (8-OHdG) levels were quantified using the OxiSelect Oxidative DNA Damage ELISA Kit (Cell Biolabs), following the manufacturer's protocol.

Statistical analyses

The data are expressed as mean and standard deviation. For the *in vitro* cell assay results, the error bars indicated the values of the standard deviations among 3 independent experiments. Statistical analyses of the differences between two groups were performed using one-way analysis of variance (ANOVA) or unpaired Student's t test. P value <0.05 is considered statistically significant.

Results

SMS2 but not SMS1 is upregulated in ovarian cancer

The protein levels of SMS1 and SMS2 were examined using both ELISA analysis and immunohistochemistry for both malignant and normal ovary tissues. To compare against malignant and normal samples, ovarian cancer tissues and their adjacent normal ovary tissues that were 1.5 cm away from the tumor were obtained from each individual patient. Patients' clinico-pathological characteristics, including age, pathological subtype, tumor grade and TNM stage, were summarized in Supplementary Table 1. A total of 30 patients diagnosed with ovarian cancer were analyzed. We found that SMS1 level was similar between normal and malignant samples (**Figure 1A**). The relative values of malignant to normal range from 0.76 to 1.4 for SMS1. In contrast, SMS2 level was increased in malignant compared to normal in majority of patients. The relative

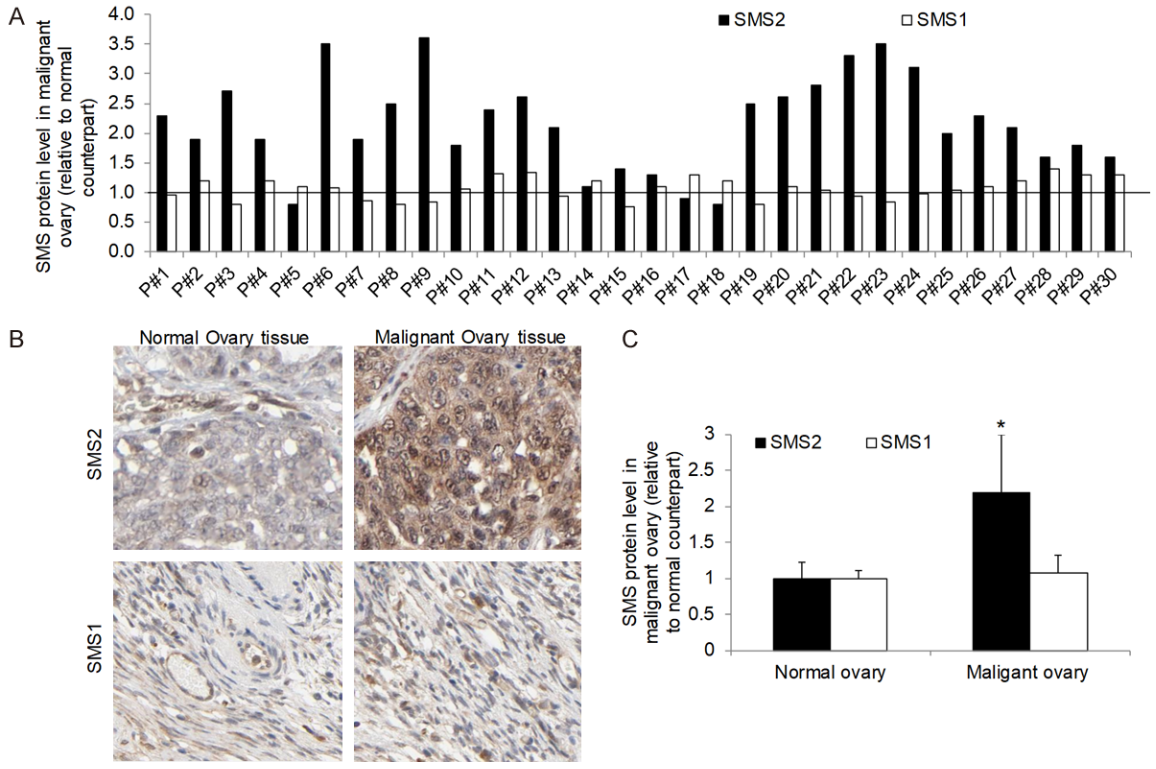

Figure 1. The expression of SMS2 but not SMS1 is upregulated in ovarian cancer. A. SMS2 but not SMS1 protein levels are higher in ovarian cancer tissues than their adjacent normal ovary tissue in the majority of patients. ELISA analysis of SMS2 and SMS1 in ovarian cancer tissues relative to normal ovary tissues. The level of SMS1 and SMS2 in ovarian cancer tissues were shown as relative to their value in adjacent normal ovary tissues in individual patient. The value of SMS1 and SMS2 in normal ovary tissues were set up as 1 (indicated by line). Total 30 different patient samples (each includes malignant and adjacent normal) were analysed. B. Representative IHC staining of SMS1 and SMS2 in patient #21 (P#21) sample shows an increase in SMS2 but not SMS1 in ovarian cancer tissues. C. The average protein level of SMS2 but not SMS1 is significantly higher in malignant than adjacent normal ovary tissues. *, P<0.05, compared to normal ovary.

value of malignant to normal was between 0.8 to 3.6 for SMS2. In addition, the upregulation of SMS2 in ovarian cancer was not associated with any clinico-pathological features (Supplementary Table 1). The expression patterns of SMS1 and SMS2 were further confirmed by immunohistochemistry as shown in **Figure 1B**. The average levels of SMS1 and SMS2 in 30 ovarian cancer patients indicated that SMS2 but not SMS1 was significantly increased in ovarian cancer than normal ovary tissues (**Figure 1C**).

SMS2 but not SMS1 is upregulated in ovarian cancer cells and SMS2 overexpression promotes growth and migration in immortalized normal ovary epithelial cells

To investigate the role of SMS2 in ovarian cancer, *in vitro* ovarian cancer and normal ovary model using cell lines were applied. These cell lines represent ovarian cancer with different histological subtypes and genetic profiling [13]. IHOEC is a human normal ovary epithelial cell immortalized with SV40 lentiviral transfection [14]. Prior to performing functional assays, we first examined whether the phenomenon observed in patients' samples is reproducible in a panel of ovarian cancer cell lines that were selected. We found that 6 of 7 ovarian cancer cell lines demonstrated higher SMS2 protein levels than IHOEC (**Figure 2A**). In contrast, ovarian cancer cells displayed similar SMS2 protein level between ovarian cancer and normal ovary cells. The upregulation of SMS2 but not SMS1 in ovarian cancer cells was not only on the protein level but also seen on the mRNA level (**Figure 2B**). We next transfected IHOEC with mammalian expression construct containing SMS2 and confirmed SMS2 overexpression

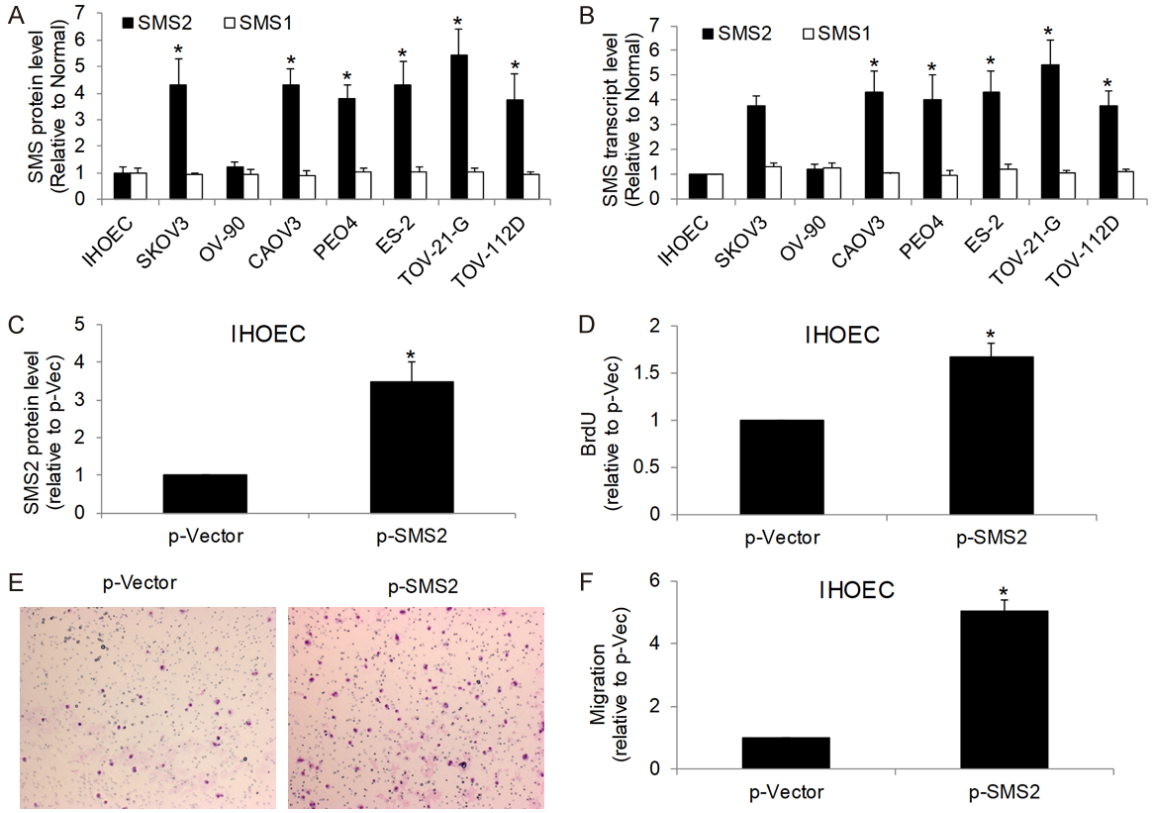

Figure 2. SMS2 overexpression promotes growth and migration in ovarian cancer cells. ELISA (A) and RT-PCR (B) analysis of SMS1 and SMS2 shows an increase in SMS2 but not SMS1 expression in ovarian cancer cells compared with normal immortalized human ovarian epithelial cells (IHOEC). Seven human ovarian cancer cell lines were used for expression analysis. (C) ELISA analysis of SMS2 level in IHOEC cells after transfection of SMS2-overexpressing plasmid shows significantly higher level of SMS2 in SMS2-overexpression IHOEC cells. (D) Significantly increased BrdU level in SMS2-overexpressing IHOEC cells. Representative transwell migration image (E) and quantification (F) of migration demonstrate significantly increased migration in SMS2-overexpressing IHOEC. The cells in five randomly selected fields were counted under a microscope. Cells at 48 h-post transfection were used for cellular assays. Cells were harvested for BrdU and migration analysis after 72 h and 12 h after seeding transfected cells to designated plates, respectively. *, $P<0.05$, compared to p-Vector.

(**Figure 2C**). We further found that SMS2 overexpression significantly increased proliferation and migration in IHOEC (**Figure 2D**, **2E**). Of note, proliferation and migration were increased by ~1.5-fold and ~5-fold respectively, suggesting that SMS2 might play a predominant role in migration rather than proliferation.

SMS2 knockdown inhibits proliferation, migration and survival, and augments cisplatin's efficacy in ovarian cancer cells

We further validated the role of SMS2 using loss-of-function approach via siRNA knockdown. We performed knockdown using two independent siRNA targeting different regions of SMS2 in OV-90 and TOV-21-G. Compared to IHOEC, OV-90 displays similar SMS2 level whereas TOV-21-G displays significantly higher SMS2 level (**Figure 2A** and **2B**). Western blot analysis confirmed that SMS2 siRNA specifically reduced SMS2 level to a minimal level and did not affect SMS1 level in both cell lines (**Figure 3A**). We found that SMS2 knockdown significantly decreased proliferation and migration, and induced apoptosis in both ovarian cancer cell lines regardless of their SMS2 baseline expression level (**Figure 3B-D** and Supplementary Figures 1, 2, 3, 4). In addition, SMS2 knockdown resulted in inhibition of growth, migration and survival in TOV-21-G that were more significant than in OV-90 cells, suggesting that TOV-21-G is more dependent on SMS2 than OV-90. Importantly, we observed significant further inhibition of growth and migration by cisplatin in SMS2-depleted cells

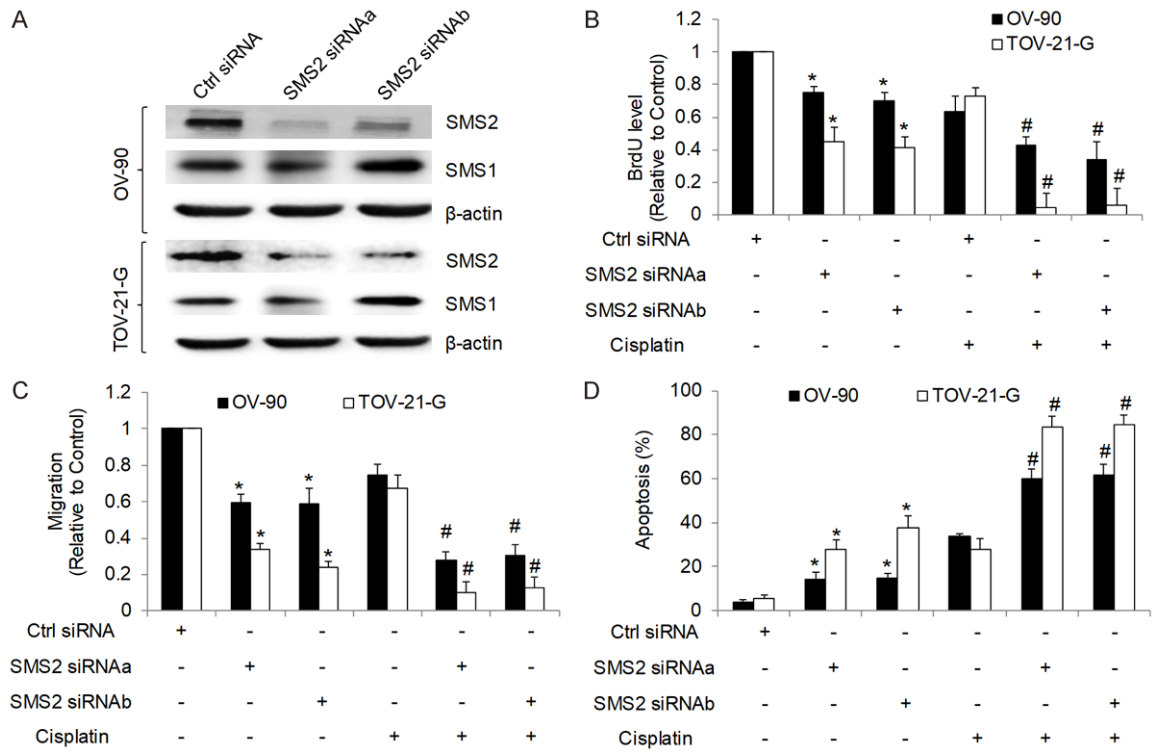

Figure 3. SMS2 knockdown inhibits ovarian cancer cells and augments cisplatin's efficacy. (A) Western blot analysis of SMS2 and SMS1 in OV-90 and TOV-21-G cells after SMS2 siRNA knockdown shows a remarkable reduction of SMS2 but not SMS1 protein levels in SMS2-depleted cells. Cells were harvested for western blot analysis at 48 h-post transfection. SMS2 siRNA knockdown significantly decreases proliferation (B) and migration (C), induces apoptosis (D) in OV-90 and TOV-21-G cells. Cisplatin treatment results in a significant further reduction of proliferation and migration in cells after SMS2 siRNA knockdown compared to control cells. Cisplatin treatment results in a significant increase of apoptosis in cells after SMS2 siRNA knockdown compared to control cells. Cells at 48 h-post transfection were used for cellular assays. Cisplatin at 50 nM was added to cells. *P<0.05, compared to Ctrl siRNA. #P<0.05, compared to cisplatin.

compared to control cells (**Figure 3B** and **3C**). Cisplatin induced ~30% apoptosis in control cells and 60% to 80% in SMS2-depleted cells (**Figure 3D**). These results clearly demonstrate that SMS2 knockdown augments cisplatin's efficacy in ovarian cancer cells.

SMS2 executes its function in ovarian cancer cells via multiple mechanisms

Small GTPases, such as RhoA and Rac1, are the known masters in cell migration [15]. Given the role of sphingomyelin metabolism in regulating activity and function of small GTPases [16, 17], we examined the active level of Rac1 and RhoA in ovarian cancer cells after SMS2 depletion. We observed a remarkable reduction of RhoA-GTP but not Rac1-GTP in SMS2-depleted cells, and that total RhoA and Rac1 were not affected in SMS2-depleted cells (**Figure 4A**). These indicate that SMS2 inhibition specifically decreases RhoA but not Rac1 activity without affecting protein expression of these GTPases. Rho-associated protein kinase (ROCK) is the downstream effector of RhoA pathway. Rho-kinase also phosphorylates myosin phosphatase-targeting subunit 1 (MYPT1) on thr853 and myosin light chain (MLC) at Ser19 to regulate cell migration [18]. Consistent with RhoA activity inhibition, SMS2 inhibition decreased the phosphorylation of MYPT1, MLC and cofilin, three downstream ROCK effectors involved in cytoskeleton reorganization [18, 19], but not protein-related kinase 2 (PRK2; **Figure 4A**). To confirm the specific role of SMS2 on RhoA activity and its-mediated signalling, we further performed RhoA activity assay and examined other molecules that are essentially involved in RhoA signalling in cells after SMS2 depletion. Consistent with our findings, we found that SMS2 depletion remarkably

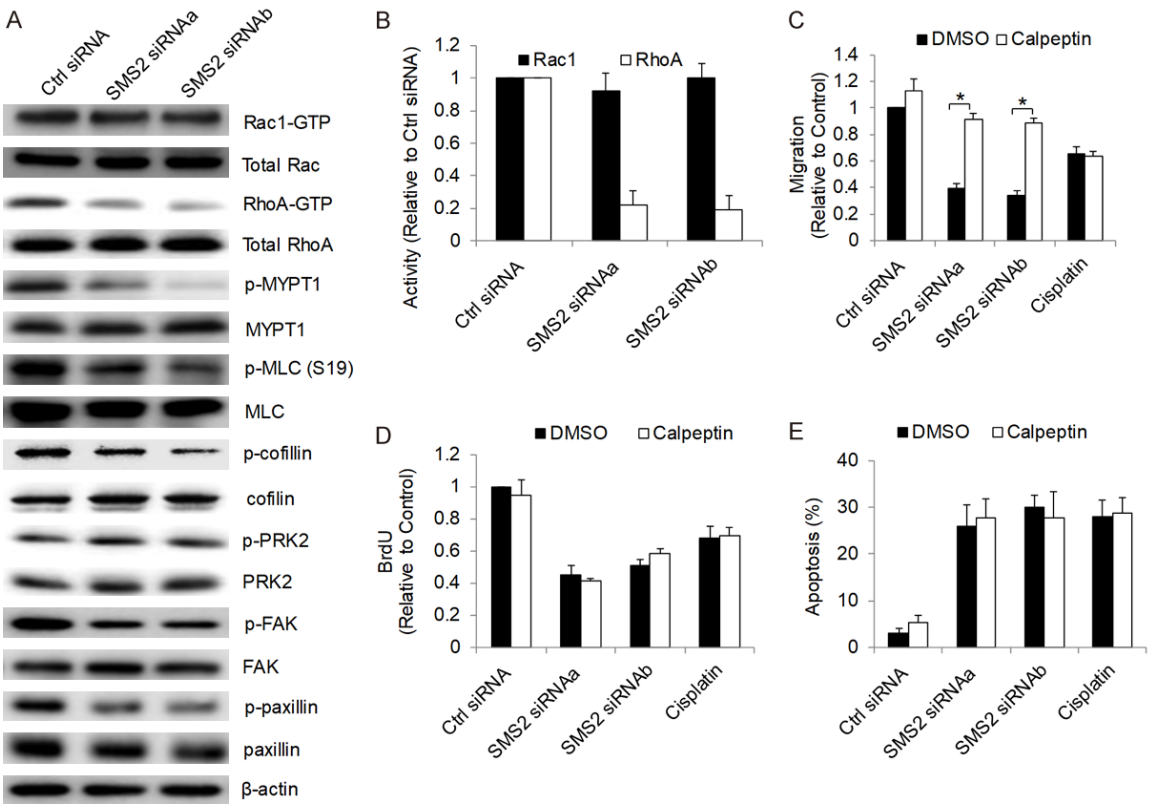

Figure 4. SMS2 depletion suppresses ovarian cancer migration via inhibiting RhoA signaling. (A) Western blot analysis of active and total Rac and RhoA, phosphor and total MYPT1, MLC, cofilin, PRK2, FAK and paxillin in SMS2-depleted TOV-21-G cells. Cells were harvested for western blot analysis at 48 h-post transfection. (B) SMS2 depletion significantly reduces the activity of RhoA but not Rac1 in TOV-21-G cells. (C) The addition of RhoA activator calpeptin significantly reverses the decreased migration in SMS2-depleted ovarian cancer cells. The addition of calpeptin does not reverse the decreased proliferation (D) and increased apoptosis (E) in SMS2-depleted ovarian cancer cells. Calpeptin at 1 mg/ml was added to the cells. Cells were harvested for BrdU and migration analysis after 72 h and 12 h after seeding transfected cells to designated plates, respectively. *, $P<0.05$, compared to Ctrl siRNA.

decreased the activity of RhoA but not Rac1 (**Figure 4B**). In addition, we further observed the decreased phophosphorylation of focal adhesion kinase (FAK) and paxillin in SMS2-depleted cells (**Figure 4A**), indicating that SMS2 inhibition also suppresses RhoA/FAK/paxillin signalling. This is consistent with the previous report that FAK/paxillin activation is mediated by RhoA/ROCK1 to regulate cytoskeletal assembly [20].

Next, we explored a link between activation of RhoA and SMS2 by attempting to rescue the effects of SMS2 inhibition using RhoA activator calpeptin [21]. We found that calpeptin significantly reversed migration inhibition induced by SMS2 depletion in ovarian cancer cells (**Figure 4B**). However, calpeptin did not reverse SMS2 depletion-induced growth and survival inhibition (**Figure 4C** and **4D**). These demonstrate that SMS2 inhibition suppresses ovarian cancer migration through suppressing RhoA signalling, and SMS2 inhibition suppresses growth and induces apoptosis through other mechanisms unrelated RhoA.

We further determined ceramide, phosphatidylcholine (PC) and sphingomyelin (SM) levels in SMS2-depleted ovarian cancer cells using LC-MS. We found that SMS2 depletion caused a slight but significant decrease of SM levels by 20% (**Figure 5A**). SMS2 depletion caused a significant increase of ceramide levels by ~1.7-fold, and did not affect PC level. We further found that SMS2 depletion resulted in an increase in intracellular ROS level (**Figure 5B**) and 8-OHdG (an oxidative DNA damage marker; **Figure 5C**), and a decrease in mitochondrial membrane potential (**Figure 5D** and Supplementary Figure 5), suggesting oxidative

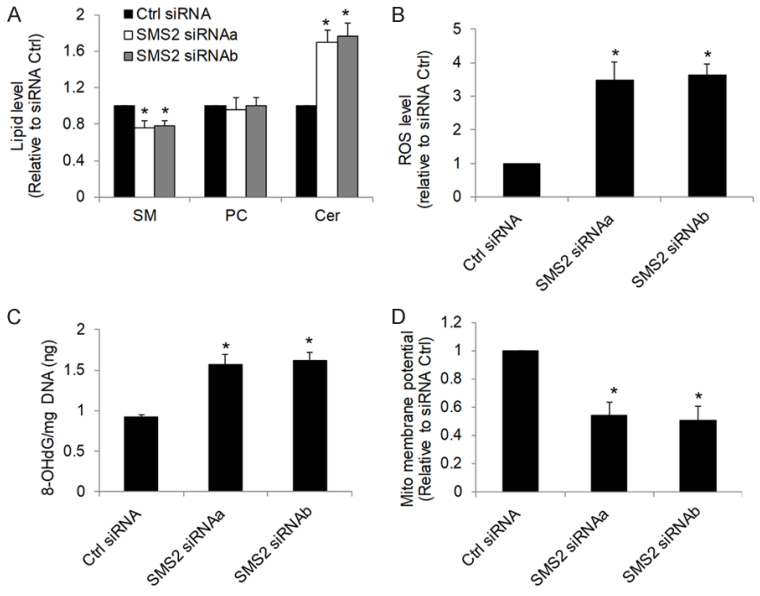

Figure 5. SMS2 depletion suppresses ovarian cancer growth and apoptosis via disrupting lipid metabolism and inducing oxidative stress. (A) SMS2 knockdown significantly increases ceramide (Cer) and deceases sphingomyelin (SM) levels without affecting phosphatidylcholine (PC) level in ovarian cancer cells. SMS2 knockdown significantly increases intracellular ROS (B) and 8-OHdG (C), and decreases mitochondrial membrane potential (D). LC-MS was applied to determine ceramide and sphingomyelin levels and differentiate distinct fatty acyl subspecies of sphingolipids. Measurement of lipids, ROS, 8-OHdG and mitochondrial membrane potential were performed at 48 h post-transfection. *, P<0.05, compared to Ctrl siRNA.

stress and mitochondrial dysfunction in cells. The disrupted lipid metabolism, oxidative damage and mitochondrial dysfunction correlates well with each other, and are likely to be the mechanisms of SMS2 depletion-induced inhibition of growth and survival in ovarian cancer cells.

Discussion

In this study, we first examined the expression patterns of both SMS1 and SMS2 in ovarian cancer in comparison with paired normal ovary tissues. SMS1 and SMS2 metabolize ceramide into SM which play critical roles in plasma membrane homeostasis and dynamics as well as in many cellular processes [6]. Although SMS are emerging as attractive therapeutic targets in cancer due to their essential roles in regulating cancer progression and treatment resistance [9, 11, 22, 23], very few studies revealed the expression pattern and prognostic value of SMS in cancer. SMS1 downregulation occurs in melanoma and is associated with a worse prognosis [24]. Interestingly, patients with high-SMS1 and low-SMS2 expression had a 5-year survival ~10-fold higher than patients with low-SMS1 and high-SMS2 expression [10], suggesting that SMS1 and SMS2 expression shows opposite associations with glioma patient survival. We showed that SMS2 expression was upregulated in most ovarian cancer patients whereas SMS1 expression remained comparable, and their expression pattern were not associated with age, pathological subtype, tumor grade, treatment and TNM stage (**Figure 1** and Supplementary Table 1). Our findings on total 30 ovarian cancer patients were consistent with RNA-sequencing data from TCGA that showed an average SMS2 mRNA level to be higher in ovarian cancer (n=350+) than normal ovary tissues (n=150+). In contrast, TCGA data demonstrates that the average SMS1 mRNA is lower in ovarian cancer (n=300+) than normal ovary tissues (n=100+). This is different from our findings that there seems to be insignificant difference on the average level of SMS1 between ovarian cancer (n=30) and ovary tissues (n=30). The reason behind may be a result of differences in samples sizes. We noted that the FPKM (fragments per kilobase million) value of SMS1 varies remarkably and a large number of ovarian cancer and ovary tissues have a similar FPKM value. Although analysis of correlation between mRNA expression level and patient survival on TCGA indicates that SMS2 is not a prognostic marker in ovarian cancer, patients with higher SMS2 expression do have lower 5-year survival rate than patients with low SMS2 expression. Furthermore, the ovarian cancer cell lines we had selected to demonstrate the biological function of SMS mimics the features of patient samples by showing that SMS2 but not SMS1 was upregulated in most ovarian cancer cell lines (**Figure 2A** and **2B**).

Based on the findings obtained from expression analysis, we investigated the function of SMS focusing on SMS2. Using gain-of-function

and loss-of-function approaches, we demonstrated that SMS2 overexpression facilitated both proliferation and migration in ovarian cancer with the predominant role in migration (**Figure 2C-F**). This is supported by previous study that SMS2 promotes breast cancer cell growth and invasiveness, and high SMS2 expression is associated with breast cancer metastasis [9]. In contrast, another study reported that SMS2 overexpression alone did not affect liver cancer cell survival but sensitized these cells to cisplatin-induced apoptosis [11]. The discrepancy on the effects of SMS2 overexpression in cancer suggest that the role of SMS2 in cancer is complex and might be cancer type specific. SMS2 depletion suppresses migration, growth and survival, and sensitizes ovarian cancer to cisplatin. Furthermore, the degree of inhibition is dependent on SMS2 baseline level in ovarian cancer cells (**Figure 3**). SMS2 deficiency inhibits the induction of colitis-associated colon cancer [25]. Loss of SMS2 inhibits the infiltration of malignant lymphoma in mice [26]. Our work together with previous reports show that SMS2 is involved in multiple aspects of cancer progression and thus is an attractive therapeutic target.

A significant finding of our work is that SMS2 contributes to ovarian cancer progression via different mechanisms. SM levels in cell plasma membrane and lipid rafts regulate function of small GTPases, such as K-Ras and RhoA [16, 17, 27]. Our findings agree with and extend the previous reports by showing that SMS2 knockdown suppresses ovarian cancer migration via inhibiting RhoA activity and its downstream signaling RhoA/ROCK/cofilin and RhoA/ROCK/FAK/paxillin pathways (**Figure 4A-C**). Inhibitors targeting ROCK/LIMK/cofilin signaling pathway have being evaluated in clinical trials for cancer treatment [19]. We are the first to demonstrate the association between SMS2 and this pathway in ovarian cancer migration. However, RhoA is not a major downstream effector of SMS2 in ovarian cancer growth and survival (**Figure 4D** and **4E**). We show that the disrupted SM metabolism (eg, increased ceramide and decreased SM), oxidative damage and mitochondrial dysfunction likely contribute to decreased growth and survival induced by SMS2 depletion (**Figure 5**). In agreement with the previous reports on the roles of SM metabolism in ovarian cancer drug resistance, microenvironment and cancer stem cell niche [7, 28], our study further highlights that SM metabolism is important for ovarian cancer growth, survival and sensitivity for cisplatin treatment.

In conclusion, our work sets the stage to evaluate the expression, function and downstream effectors of SMS in ovarian cancer. Our work demonstrates that that SMS2 but not SMS1 is upregulated in ovarian cancer, and involved in migration, growth and survival via different mechanisms. These discoveries are critical preclinical steps towards investigating SMS2 pharmacological inhibitors in combinations with existing treatment measures to achieve chemo-sensitization in ovarian cancer.

Acknowledgements

This work was supported by Wuhan Health and Family Commission Project (No. WX18D22).

Disclosure of conflict of interest

None.

Address correspondence to: Li Hong, Department of Gynecology, Renmin Hospital of Wuhan University, No.238 Jiefang Road, Wuchang District, Wuhan 430060, Hubei, China. E-mail: drhongli771@163.com

References

[1] Zhang Y, Luo G, Li M, Guo P, Xiao Y, Ji H and Hao Y. Global patterns and trends in ovarian cancer incidence: age, period and birth cohort analysis. BMC Cancer 2019; 19: 984.

[2] Koshiyama M, Matsumura N and Konishi I. Subtypes of ovarian cancer and ovarian cancer screening. Diagnostics (Basel) 2017; 7: 12.

[3] Grabowski JP and Sehouli J. Current management of ovarian cancer. Minerva Med 2015; 106: 151-156.

[4] Agarwal R and Kaye SB. Ovarian cancer: strategies for overcoming resistance to chemotherapy. Nat Rev Cancer 2003; 3: 502-516.

[5] D'Angelo G, Moorthi S and Luberto C. Role and function of sphingomyelin biosynthesis in the development of cancer. Adv Cancer Res 2018; 140: 61-96.

[6] Ogretmen B. Sphingolipid metabolism in cancer signalling and therapy. Nat Rev Cancer 2018; 18: 33-50.

[7] Kreitzburg KM, van Waardenburg R and Yoon KJ. Sphingolipid metabolism and drug resistance in ovarian cancer. Cancer Drug Resist 2018; 1: 181-197.

[8] Yeang C, Ding T, Chirico WJ and Jiang XC. Subcellular targeting domains of sphingomyelin

synthase 1 and 2. Nutr Metab (Lond) 2011; 8: 89.
[9] Zheng K, Chen Z, Feng H, Chen Y, Zhang C, Yu J, Luo Y, Zhao L, Jiang X and Shi F. Sphingomyelin synthase 2 promotes an aggressive breast cancer phenotype by disrupting the homoeostasis of ceramide and sphingomyelin. Cell Death Dis 2019; 10: 157.
[10] Fernandez-Garcia P, Rossello CA, Rodriguez-Lorca R, Beteta-Gobel R, Fernandez-Diaz J, Llado V, Busquets X and Escriba PV. The opposing contribution of SMS1 and SMS2 to glioma progression and their value in the therapeutic response to 2OHOA. Cancers (Basel) 2019; 11: 88.
[11] Luo S, Pan Z, Liu S, Yuan S and Yan N. Sphingomyelin synthase 2 overexpression promotes cisplatin-induced apoptosis of HepG2 cells. Oncol Lett 2018; 15: 483-488.
[12] Li Z, Hailemariam TK, Zhou H, Li Y, Duckworth DC, Peake DA, Zhang Y, Kuo MS, Cao G and Jiang XC. Inhibition of sphingomyelin synthase (SMS) affects intracellular sphingomyelin accumulation and plasma membrane lipid organization. Biochim Biophys Acta 2007; 1771: 1186-1194.
[13] Beaufort CM, Helmijr JC, Piskorz AM, Hoogstraat M, Ruigrok-Ritstier K, Besselink N, Murtaza M, van IJcken WF, Heine AA, Smid M, Koudijs MJ, Brenton JD, Berns EM and Helleman J. Ovarian cancer cell line panel (OCCP): clinical importance of in vitro morphological subtypes. PLoS One 2014; 9: e103988.
[14] Shin HY, Yang W, Lee EJ, Han GH, Cho H, Chay DB and Kim JH. Establishment of five immortalized human ovarian surface epithelial cell lines via SV40 T antigen or HPV E6/E7 expression. PLoS One 2018; 13: e0205297.
[15] Sadok A and Marshall CJ. Rho GTPases: masters of cell migration. Small GTPases 2014; 5: e29710.
[16] Abe M, Makino A, Hullin-Matsuda F, Kamijo K, Ohno-Iwashita Y, Hanada K, Mizuno H, Miyawaki A and Kobayashi T. A role for sphingomyelin-rich lipid domains in the accumulation of phosphatidylinositol-4,5-bisphosphate to the cleavage furrow during cytokinesis. Mol Cell Biol 2012; 32: 1396-1407.
[17] Saslowsky DE, Thiagarajah JR, McCormick BA, Lee JC and Lencer WI. Microbial sphingomyelinase induces RhoA-mediated reorganization of the apical brush border membrane and is protective against invasion. Mol Biol Cell 2016; 27: 1120-1130.
[18] Aburima A, Wraith KS, Raslan Z, Law R, Magwenzi S and Naseem KM. cAMP signaling regulates platelet myosin light chain (MLC) phosphorylation and shape change through targeting the RhoA-Rho kinase-MLC phosphatase signaling pathway. Blood 2013; 122: 3533-3545.
[19] Lee MH, Kundu JK, Chae JI and Shim JH. Targeting ROCK/LIMK/cofilin signaling pathway in cancer. Arch Pharm Res 2019; 42: 481-491.
[20] Zeng Y, Cao Y, Liu L, Zhao J, Zhang T, Xiao L, Jia M, Tian Q, Yu H, Chen S and Cai Y. SEPT9_i1 regulates human breast cancer cell motility through cytoskeletal and RhoA/FAK signaling pathway regulation. Cell Death Dis 2019; 10: 720.
[21] Schoenwaelder SM and Burridge K. Evidence for a calpeptin-sensitive protein-tyrosine phosphatase upstream of the small GTPase Rho. A novel role for the calpain inhibitor calpeptin in the inhibition of protein-tyrosine phosphatases. J Biol Chem 1999; 274: 14359-14367.
[22] Liu S, Hou H, Zhang P, Wu Y, He X, Li H and Yan N. Sphingomyelin synthase 1 regulates the epithelialtomesenchymal transition mediated by the TGFbeta/Smad pathway in MDAMB231 cells. Mol Med Rep 2019; 19: 1159-1167.
[23] Moorthi S, Burns TA, Yu GQ and Luberto C. Bcr-Abl regulation of sphingomyelin synthase 1 reveals a novel oncogenic-driven mechanism of protein up-regulation. FASEB J 2018; 32: 4270-4283.
[24] Bilal F, Montfort A, Gilhodes J, Garcia V, Riond J, Carpentier S, Filleron T, Colacios C, Levade T, Daher A, Meyer N, Andrieu-Abadie N and Segui B. Sphingomyelin synthase 1 (SMS1) down-regulation is associated with sphingolipid reprogramming and a worse prognosis in melanoma. Front Pharmacol 2019; 10: 443.
[25] Ohnishi T, Hashizume C, Taniguchi M, Furumoto H, Han J, Gao R, Kinami S, Kosaka T and Okazaki T. Sphingomyelin synthase 2 deficiency inhibits the induction of murine colitis-associated colon cancer. FASEB J 2017; 31: 3816-3830.
[26] Taniguchi M, Ueda Y, Matsushita M, Nagaya S, Hashizume C, Arai K, Kabayama K, Fukase K, Watanabe K, Wardhani LO, Hayashi K and Okazaki T. Deficiency of sphingomyelin synthase 2 prolongs survival by the inhibition of lymphoma infiltration through ICAM-1 reduction. FASEB J 2020; 34: 3838-3854.
[27] van der Hoeven D, Cho KJ, Zhou Y, Ma X, Chen W, Naji A, Montufar-Solis D, Zuo Y, Kovar SE, Levental KR, Frost JA, van der Hoeven R and Hancock JF. Sphingomyelin metabolism is a regulator of K-Ras function. Mol Cell Biol 2018; 38: 3.
[28] Xu Y. Lysophospholipid signaling in the epithelial ovarian cancer tumor microenvironment. Cancers (Basel) 2018; 10: 227.

Supplementary Table 1. Ovarian cancer patients' clinic-pathological data

Patient Number	Age	Grade	Histology	TNM stage
P#1	56	3	Serous papillary	II
P#2	60	3	Serous	III
P#3	33	3	Serous papillary	II
P#4	55	3	Serous papillary	IIA
P#5	65	1A	Serous	I
P#6	68	2	Serous	III
P#7	55	2	Serous papillary	III
P#8	38	3	Serous	II
P#9	39	2	Clear cell	II
P#10	49	2	Serous	III
P#11	42	2	Clear cell	III
P#12	55	1A	Serous	I
P#13	68	2A	Serous	I
P#14	72	3	Serous	II
P#15	58	2-3	Endometrioid	IIIc
P#16	76	2	Clear cell	III
P#17	79	3	Endometrioid	III
P#18	55	3	Endometrioid	II
P#19	44	3	Serous	IIa
P#20	80	3	Serous	IV
P#21	63	3	Serous	IV
P#22	64	2-3	Serous	IIIc
P#23	61	1	Serous	I
P#24	51	2	Serous	Ib
P#25	44	2	Endometrioid	Ib
P#26	38	3	Clear cell	IIIc
P#27	39	3	Clear cell	III
P#28	65	2	Clear cell	Ib
P#29	68	1	Serous	I
P#30	63	1	Serous	I

Supplementary Table 2. siRNA sequences for SGMS2

	siRNA sequence
SMS2 siRNAa	5'-AAC CCA AGA GCT TAT CCA GTC-3'
SMS2 siRNAb	5'-ACC GTC ATG ATC ACA TCC GTA-3'

Supplementary Table 3. RT-PCR primer sequences for human genes

Gene	RT-PCR primer sequence
SMS1	F: 5'-GCC AGG ACT TGA TCA ACC TAA CC-3'
	R: 5'-CCA TTG GCA TGG CCG TTC TTG-3'
SMS2	F: 5'-CTT AGC CCT CCA CTC CC-3'
	R: 5'-CAG AAT CTG CGT CCC AC-3'
GAPDH	F: 5'-AAC GGG AAG CTT GTC ATC AAT GGA AA-3'
	R: 5'-GCA TCA GCA GAG GGG GCA GAG-3'

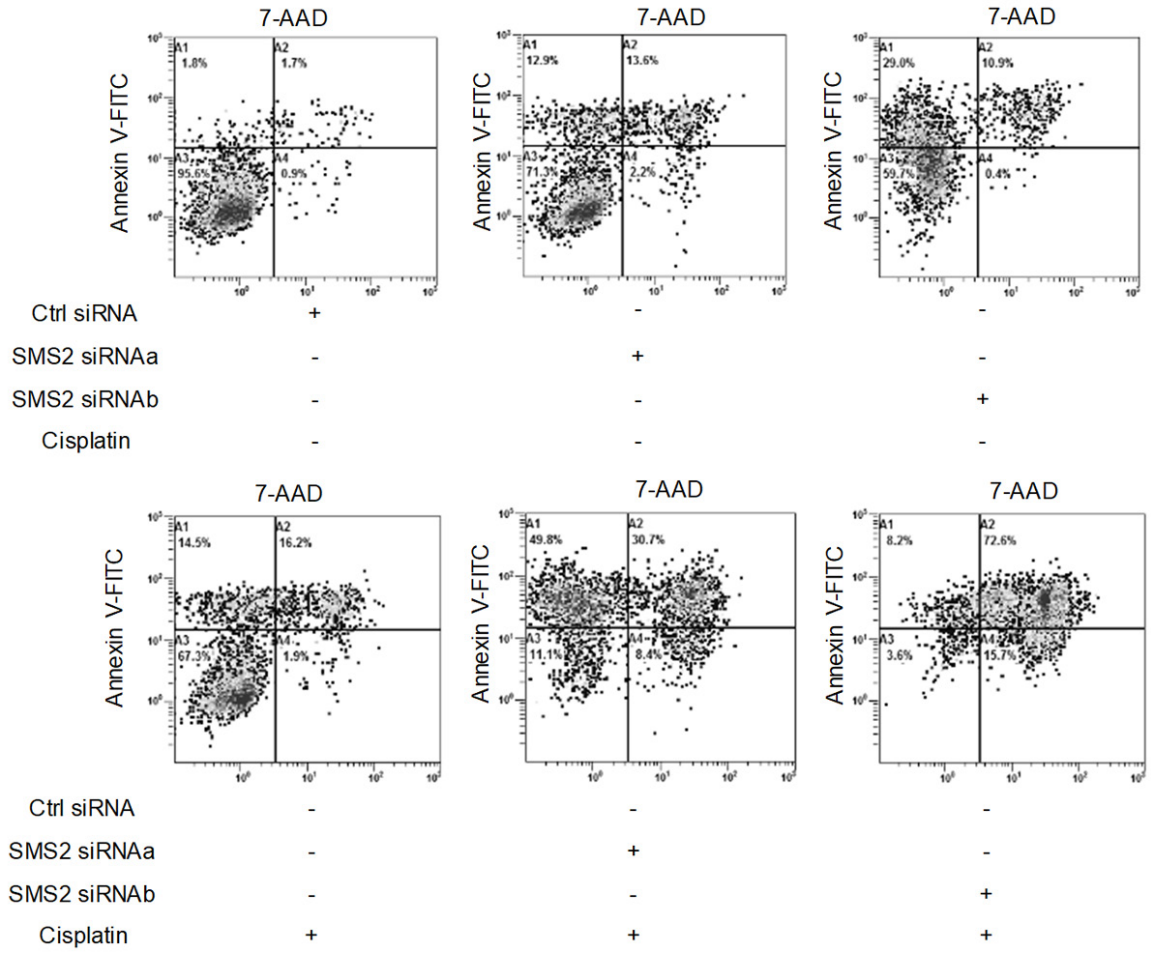

Supplementary Figure 1. Representative flow cytometry plots showing the percentage of Annexin V and 7-AAD staining in SMS2-depleted OV-90 cells in the presence of cisplatin.

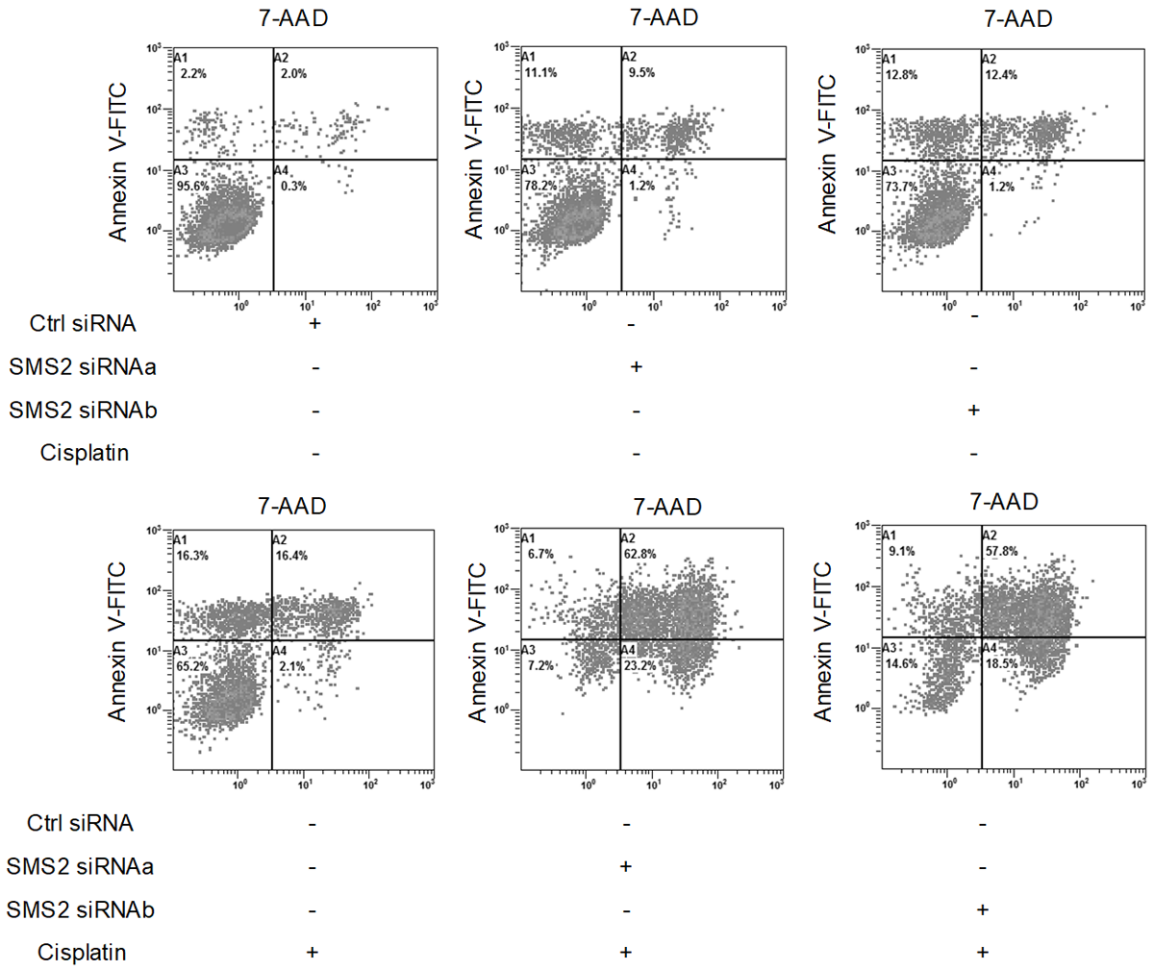

Supplementary Figure 2. Representative flow cytometry plots showing the percentage of Annexin V and 7-AAD staining in SMS2-depleted TOV-21-G cells in the presence of cisplatin.

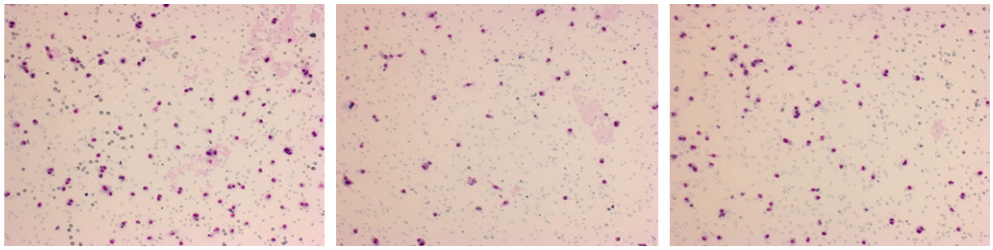

Ctrl siRNA	+	-	-
SMS2 siRNAa	-	+	-
SMS2 siRNAb	-	-	+
Cisplatin	-	-	-

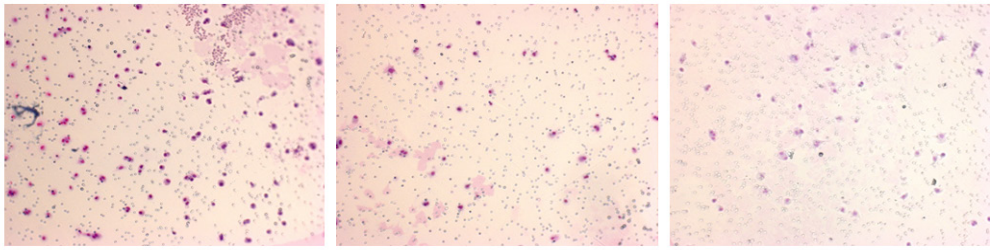

Ctrl siRNA	+	-	-
SMS2 siRNAa	-	+	-
SMS2 siRNAb	-	-	+
Cisplatin	-	-	-

Supplementary Figure 3. Representative migration images showing that SMS2 siRNA knockdown decreases migration in OV-90 cells. Cisplatin treatment results in a significant further reduction of proliferation and migration in cells after SMS2 siRNA knockdown compared to control cells.

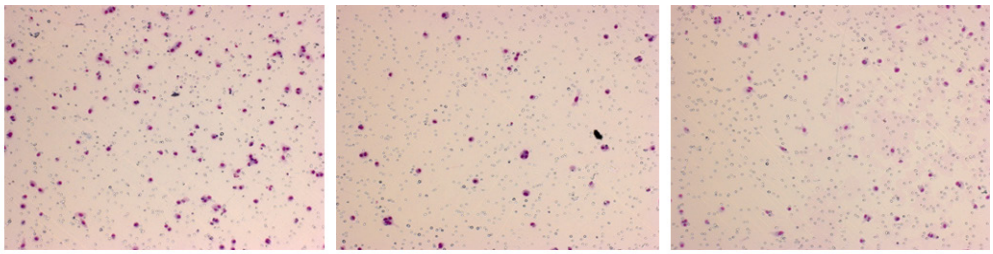

Ctrl siRNA	+	-	-
SMS2 siRNAa	-	+	-
SMS2 siRNAb	-	-	+
Cisplatin	-	-	-

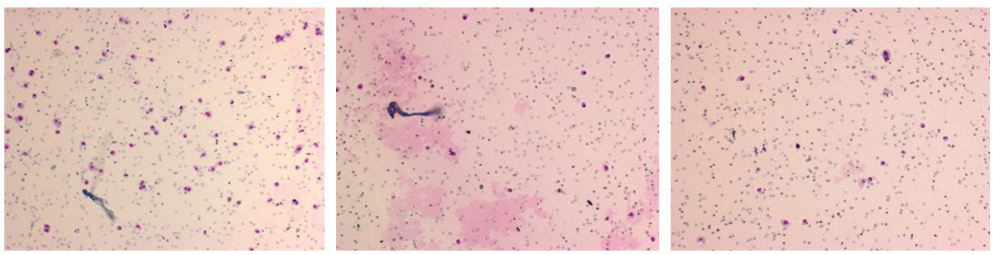

Ctrl siRNA			
SMS2 siRNAa	-	+	-
SMS2 siRNAb	-	-	+
Cisplatin	-	-	-

Supplementary Figure 4. Representative migration images showing that SMS2 siRNA knockdown decreases migration in TOV-21-G cells. Cisplatin treatment results in a significant further reduction of proliferation and migration in cells after SMS2 siRNA knockdown compared to control cells.

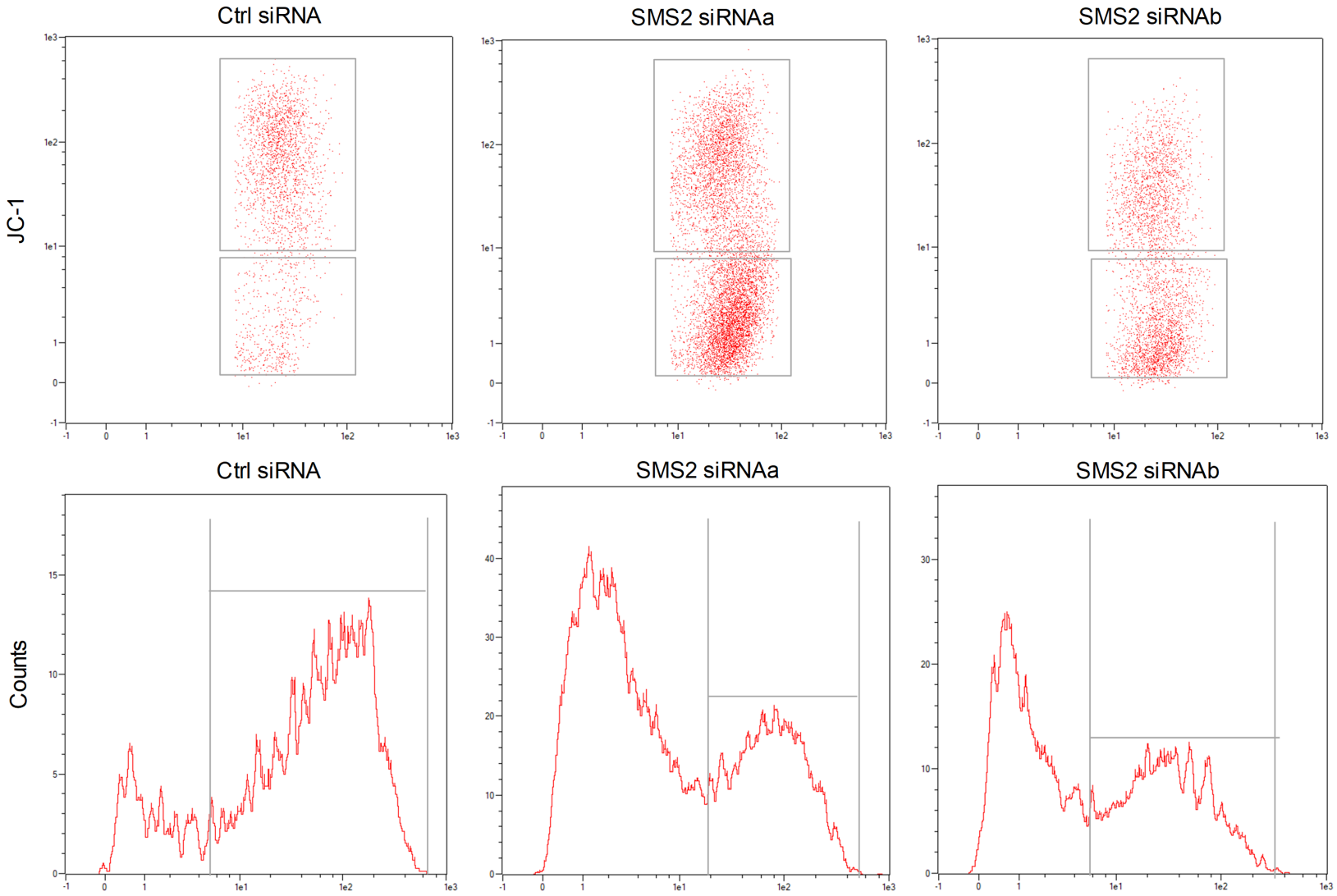

Supplementary Figure 5. Representative flow cytometry plot and histogram images showing that SMS2 siRNA knockdown decreases JC-1 staining counts.